Small-molecule allosteric activators of PDE4 long form cyclic AMP phosphodiesterases

Faisa Omar[a], Jane E. Findlay[a], Gemma Carfray[a], Robert W. Allcock[a,b], Zhong Jiang[a,b], Caitlin Moore[a], Amy L. Muir[a], Morgane Lannoy[c], Bracy A. Fertig[d], Deborah Mai[e], Jonathan P. Day[f], Graeme Bolger[g], George S. Baillie[d], Erik Schwiebert[e], Enno Klussmann[h,i], Nigel J. Pyne[j], Albert C. M. Ong[c], Keith Bowers[a,j], Julia M. Adam[a], David R. Adams[a,b], Miles D. Houslay[a,k,1], and David J. P. Henderson[a,j,1,2]

[a]Mironid, Ltd., Newhouse, North Lanarkshire ML1 5UH, Scotland, United Kingdom; [b]Institute of Chemical Sciences, Heriot-Watt University, Edinburgh EH14 4AS, United Kingdom; [c]Academic Nephrology Unit, Department of Infection Immunity and Cardiovascular Disease, University of Sheffield Medical School, Sheffield S10 2RX, United Kingdom; [d]Institute of Cardiovascular and Medical Sciences, University of Glasgow, Glasgow G12 8QQ, United Kingdom; [e]DiscoveryBioMed, Inc., Birmingham, AL 35242; [f]Department of Genetics, University of Cambridge, CB2 3EH Cambridge, United Kingdom; [g]Department of Medicine, University of Alabama at Birmingham, Birmingham, AL 35294-3300; [h]Max-Delbrück-Centrum für Molekulare Medizin, 13092 Berlin, Germany; [i]Charité–Universitätsmedizin Berlin, Corporate Member of Freie Universität Berlin, Humboldt-Universität zu Berlin, and Berlin Institute of Health, Institut für Vegetative Physiologie, 10117 Berlin, Germany; [j]Strathclyde Institute of Pharmacy and Biomedical Sciences, University of Strathclyde, Glasgow G1 1XQ, Scotland, United Kingdom; and [k]School of Cancer and Pharmaceutical Sciences, King's College London, London SE1 9NH, United Kingdom

Edited by Joseph A. Beavo, University of Washington School of Medicine, Seattle, WA, and approved May 23, 2019 (received for review January 3, 2019)

Cyclic AMP (cAMP) phosphodiesterase-4 (PDE4) enzymes degrade cAMP and underpin the compartmentalization of cAMP signaling through their targeting to particular protein complexes and intracellular locales. We describe the discovery and characterization of a small-molecule compound that allosterically activates PDE4 long isoforms. This PDE4-specific activator displays reversible, noncompetitive kinetics of activation (increased V_{max} with unchanged K_m), phenocopies the ability of protein kinase A (PKA) to activate PDE4 long isoforms endogenously, and requires a dimeric enzyme assembly, as adopted by long, but not by short (monomeric), PDE4 isoforms. Abnormally elevated levels of cAMP provide a critical driver of the underpinning molecular pathology of autosomal dominant polycystic kidney disease (ADPKD) by promoting cyst formation that, ultimately, culminates in renal failure. Using both animal and human cell models of ADPKD, including ADPKD patient-derived primary cell cultures, we demonstrate that treatment with the prototypical PDE4 activator compound lowers intracellular cAMP levels, restrains cAMP-mediated signaling events, and profoundly inhibits cyst formation. PDE4 activator compounds thus have potential as therapeutics for treating disease driven by elevated cAMP signaling as well as providing a tool for evaluating the action of long PDE4 isoforms in regulating cAMP-mediated cellular processes.

PDE4 | PDE4 activator | cyclic AMP | ADPKD | phosphodiesterase

Cyclic AMP (cAMP) is a pivotal and ubiquitous second messenger that controls the functioning of a wide spectrum of key biological processes. The functional attributes of cAMP are mediated by distinct effector systems; namely, the archetypal signaling system provided by protein kinase A (PKA) (1) together with the more recently discovered systems provided by exchange factor activated by cAMP (Epac) (2, 3) and the so-called POPEYE proteins (4). cAMP homeostasis is effected by an interplay of synthesis, determined by members of a multigene family of adenylyl cyclases, and degradation, via a multigene family of cyclic nucleotide phosphodiesterases (PDEs) (5–7).

Of particular importance in this are isoforms of the four-gene (A/B/C/D) cAMP phosphodiesterase-4 (PDE4) family. The use of PDE4-selective inhibitors, PDE4 gene-knockout studies, dominant-negative approaches, and genetic analyses have identified the cAMP-specific PDE4 family as playing a pivotal role in regulating a wide variety of key physiological processes and in underpinning the molecular pathology of various diseases (8–12). The therapeutic potential of manipulating PDE4 activity is clearly demonstrated by selective inhibitors acting as antiinflammatory agents and recently adopted for clinical use in the treatment of psoriasis, psoriatic arthritis, and chronic obstructive pulmonary disease (COPD) (5, 13–15).

PDE4 isoform heterogeneity allows for their differential regulation through cross-talk and feedback processes together with a distinct critical spatial component, achieved by targeting of isoforms to specific cellular signaling complexes (8). In this way, targeted degradation by spatially discrete PDE4 isoforms plays a major role in underpinning the compartmentalization of intracellular cAMP signal transduction by forming and shaping intracellular pools/gradients of cAMP that are able to modulate distinct cellular processes (8).

PDE4 isoforms are grouped into four categories. These are long isoforms, which possess both of the regulatory upstream conserved region 1 (UCR1) and upstream conserved region 2 (UCR2) domains; short forms, which lack UCR1; supershort forms, which both lack UCR1 and have a truncated UCR2; and dead-short forms, which lack both UCR1 and UCR2 as well as have a truncated catalytic unit that renders them catalytically

Significance

Cyclic AMP (cAMP) is a universal second messenger found in cells of all biological systems. In mammalian cells, it controls critical actions as diverse as cardiac function, cell proliferation, learning, and memory, for example. Even within a cell, it can differentially control distinct processes by virtue of compartmentalization, where targeted degradation by cAMP phosphodiesterases (PDEs) forms and shapes gradients that underpin this spatiotemporal organization. Here, we describe a small-molecule allosteric activator of PDE4 long isoforms. This discovery is poised to have considerable impact for both developing therapeutics and as a probe for gaining insight into the impact of PDE4 long isoforms upon the fundamental cellular processes that cAMP controls in health and disease.

Author contributions: K.B., J.M.A., D.R.A., M.D.H., and D.J.P.H. designed research; F.O., J.E.F., G.C., R.W.A., Z.J., C.M., A.L.M., M.L., B.A.F., D.M., J.P.D., and E.S. performed research; G.B. and N.J.P. contributed new reagents/analytic tools; J.P.D., G.S.B., E.S., E.K., A.C.M.O., K.B., J.M.A., D.R.A., M.D.H., and D.J.P.H. analyzed data; and M.D.H. and D.J.P.H. wrote the paper.

Conflict of interest statement: D.J.P.H., F.O., J.E.F., R.W.A., Z.J., G.C., C.M., A.L.M., K.B., J.M.A., D.R.A., and M.D.H. are employees of Mironid, Limited. N.J.P., E.K., and A.C.M.O. act as consultants to Mironid, Limited.

This article is a PNAS Direct Submission.

[1]M.D.H. and D.J.P.H. contributed equally to this work.

[2]To whom correspondence may be addressed. Email: david.henderson@mironid.com.

This article contains supporting information online at www.pnas.org/lookup/suppl/doi:10.1073/pnas.1822113116/-/DCSupplemental.

Published online June 17, 2019.

inactive (9, 12). These various UCR1/2 combinations confer distinct differences in the ability of PDE4 isoforms to be regulated by phosphorylation through the action of a variety of protein kinases, allowing PDE4 isoforms to serve as key nodes for integrating responses between different signaling pathways (8, 16). In particular, UCR1-targeted phosphorylation, with concomitant activation, of PDE4 long isoforms by PKA provides a pivotal component of the cellular cAMP signaling desensitization system (17). Such functionality requires only a relatively small increase (~30–100% range) in the cAMP degrading activity of PDE4 long isoforms to exert a profound effect on diminishing cellular cAMP levels (17–19). Furthermore, MK2 [MAP kinase-activated protein kinase 2 (MAPKAPK2)], the key downstream kinase of the p38 MAP kinase inflammatory pathway, also phosphorylates PDE4 long isoforms, thereby achieving subtle inhibitory manipulation of the level of activation of PDE4 long isoforms conferred by PKA phosphorylation (18).

Interestingly, PDE4 long isoforms, but not short isoforms, show similar levels of activation in response to the binding of phosphatidic acid to UCR1 (20) and the binding of a short "UCR1-related" peptide (UCR1C), which has been suggested to function by disrupting the interaction between the UCR1 and UCR2 (21). Thus, long, but not short, isoforms from all four PDE4 subfamilies have an inherent ability to be activated endogenously through a variety of routes. Such activation appears to involve the UCR1 regulatory domain and requires the enzyme to adopt a dimeric conformation (22). This particular quaternary structural status is uniquely associated with long PDE4 isoforms because two key dimerization interfaces are involved, one located within the catalytic domain and the other involving the long-form–specific UCR1 domain (23).

Here, we describe a drug-like compound that allosterically activates long, but not short, PDE4 isoforms. This PDE4-selective long-isoform activator demonstrably lowers intracellular cAMP levels leading to reduced PKA activity. Compounds exerting such functional effects may have utility in treating diseases where chronically elevated cAMP levels drive the molecular pathology. Indeed, using in vitro kidney cell models of one such disease, namely autosomal dominant polycystic kidney disease (ADPKD), where chronically elevated cAMP levels drive cyst formation (24–28), we show that the PDE4 activator compound MR-L2 inhibits cyst formation.

Results

Small-Molecule Activators of Long-Form PDE4 Isoforms. During the course of a chemistry program to develop PDE4 structure–function probes and PDE4-selective inhibitors, we uncovered a substituted triazole compound able to activate PDE4 long isoforms in a concentration-dependent manner. Taking this compound as a starting point, we then embarked upon a campaign to develop additional PDE4 activators as tool compounds with which to further investigate their biological effects in vitro and assess their therapeutic potential. This resulted in the generation of a series of small-molecule PDE4 activators, exemplified by MR-L2 in Fig. 1*A* (additional examples in *SI Appendix*, Fig. S1).

Four distinct genes (*PDE4A*, *PDE4B*, *PDE4C*, and *PDE4D*) encode the PDE4 family of enzymes (8–10, 12, 29). As well as being separated into four distinct gene families, catalytically active PDE4 isoforms can be segregated into long, short, and supershort isoform variants based upon the presence (or absence) of so-called UCR1 and UCR2 sequences (Fig. 2*A*) (9, 29). MR-L2 (Fig. 1*A*), similarly activates representative PDE4 long-isoform variants (PDE4A4, PDE4B1, PDE4C3, PDE4D5) from each of the four PDE4 genes (Fig. 1*B* and *SI Appendix*, Fig. S2*A*), albeit with a slightly enhanced magnitude of activation observed for PDE4A4. Thus, for example, the commonly expressed PDE4D5 isoform exhibited a ~60% increase in activity over basal levels at maximally effective concentrations of MR-L2. This is of a similar magnitude to the level of endogenous activation of PDE4D5 by PKA that elicits profound down-regulation of cAMP (17, 29). As might be predicted, the stimulatory effects are specific to the PDE4 family, as demonstrated by the failure of MR-L2 to enhance the activity of exemplars from any of the other 10 families within the PDE superfamily (*SI Appendix*, Fig. S2*B*).

The Activation of PDE4 Long Isoforms Mirrors Activation by PKA Phosphorylation. Interestingly, the magnitude of PDE4 long-form activation by MR-L2 (Fig. 1*B*) is comparable to the degree of activation observed when PDE4 long isoforms are activated by the PKA-mediated phosphorylation of a conserved serine located within the UCR1 domain that is unique to long PDE4 isoforms and absent from short/supershort isoforms (17, 19, 30, 31) (Fig. 2*A* and *SI Appendix*, Fig. S2*C*). This suggested to us that the activator

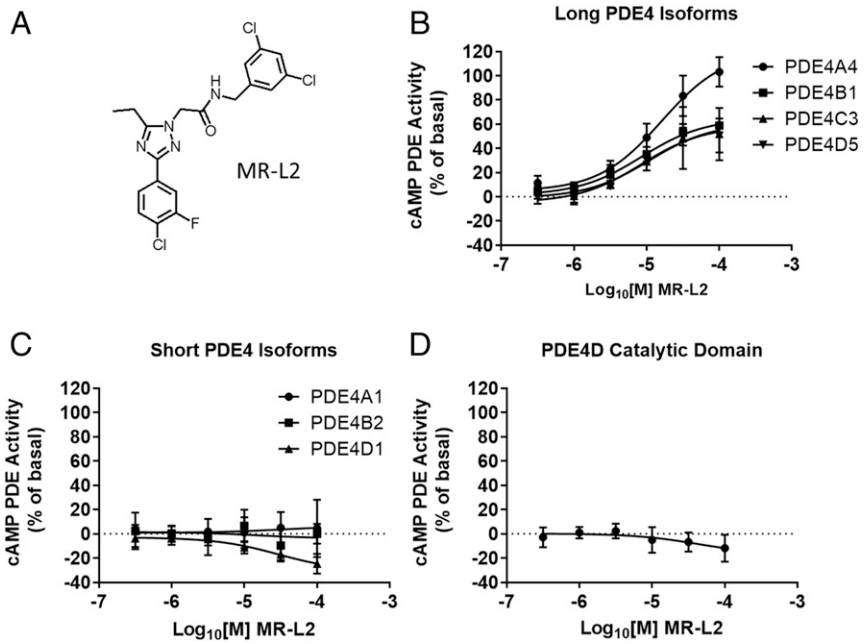

Fig. 1. Exemplar long-form PDE4 activator compound series. (*A*) An *N*-substituted-2-(3-aryl-1*H*-1,2,4-triazol-1-yl)acetamide chemotype was identified with long-form PDE4 activation properties, as exemplified here with 2-(3-(4-chloro-3-fluorophenyl)-5-ethyl-1*H*-1,2,4-triazol-1-yl)-*N*-(3,5-dichlorobenzyl)acetamide (MR-L2). (*B*) MR-L2 activates representative long-form PDE4 enzymes from each PDE4 family. Error bars represent SD of at least four independent experiments. (*C*) MR-L2 did not activate exemplar short isoforms of PDE4A, B, and D families (PDE4C expresses no short-form variants). (*D*) MR-L2 does not activate an engineered construct expressing a truncated core catalytic domain of PDE4D without UCR1, UCR2, and C-terminal tail. Data from $n = 4$ separate experiments shown as mean ± SD.

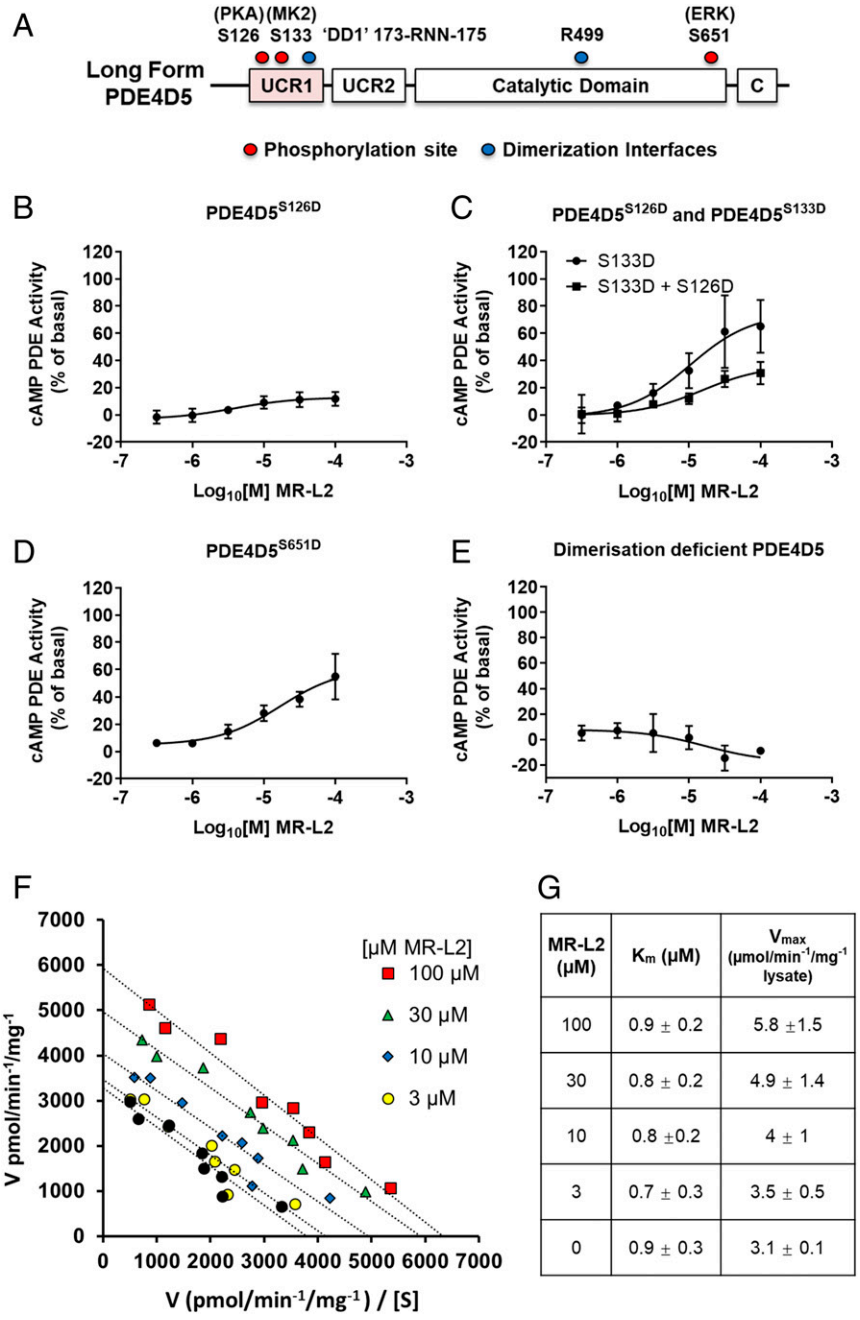

MR-L2 (μM)	K_m (μM)	V_{max} (μmol/min^{-1}/mg^{-1} lysate)
100	0.9 ± 0.2	5.8 ±1.5
30	0.8 ± 0.2	4.9 ± 1.4
10	0.8 ±0.2	4 ± 1
3	0.7 ± 0.3	3.5 ± 0.5
0	0.9 ± 0.3	3.1 ± 0.1

Fig. 2. PDE4 activator treatment phenocopies PKA-mediated activation of long PDE4 isoforms. (*A*) A schematic diagram of PDE4 that details the mutations used to investigate the action of MR-L2 on the long PDE4 isoform, PDE4D5. (*B*) A S126D phosphomimetic substitution was used as a surrogate for PKA phosphorylation. The S126D mimetic construct is not activated by MR-L2, indicating that the activated long-form PDE4 state engendered by the mutation is insensitive to further pharmacological activation. (*C*) S133D was engineered as a surrogate for MKII phosphorylation of PDE4D5. Alone, the S133D substitution does not affect the activation of PDE4D5 by MR-L2. However, when engineered in combination with the PKA phosphomimetic, the S133D partially restores the sensitivity to pharmacological activation of the A S126D mutant enzyme. (*D*) The phosphorylation of PDE4D5 by Erk was similarly simulated by introducing a S651D mutation. MR-L2 activated this construct, indicating that the activator can overcome Erk phosphorylation-mediated inhibition of long-form PDE4 activity. (*E*) A dimerization-deficient mutant of PDE4D5 (DD1-R499D-PDE4D5) is unable to be activated by MR-L2. (*F*) Eadie Hofstee analysis of enzyme velocity showing the pharmacological activation of PDE4D5 with 3, 10, 30, and 100 μM MR-L2. The activator compound increases PDE4D5 V_{max} without changing K_m for cAMP. (*G*) Average V_{max} and K_m values calculated from $n = 4$ independent experiments ± SD.

compounds may phenocopy the PKA activation process. Indeed, such levels of activation are physiologically relevant, providing a major regulatory mechanism in terms of PKA-mediated feedback allowing desensitization to cAMP signaling in PDE4 long-isoform–expressing cells (17, 18). This feedback exerts a major impact on the magnitude and duration of elevation of cAMP levels in cells subsequent to the activation of adenylyl cyclase (16–18, 32, 33). In contrast to its ability to activate PDE4 long isoforms, MR-L2 failed to activate short PDE4 isoforms, which lack the regulatory UCR1 domain and so are insensitive to activation by PKA (Fig. 1*C*). Moreover, the compound failed to activate engineered PDE4 species that comprise solely a core, functional catalytic unit deprived of both the regulatory UCR1 and UCR2 domains and the C-terminal domain (Fig. 1*D*), again highlighting the requirement for protein domains distal to the catalytic site in pharmacological activation of PDE4 species. Furthermore, if the stimulatory effects of the activator compound phenocopy the activation process engendered by PKA phosphorylation of long PDE4 isoforms, then such actions should not be additive. It is possible to mimic the PKA phosphorylated state of PDE4 long isoforms by engineering a Ser:Asp swap in the "Arg–Arg–Glu–Ser–Phe" PKA consensus motif conserved in the UCR1 region of all PDE4 long isoforms (Fig. 2*A*) (19, 30). The advantage of using such a mutant species is that it ensures that the entire PDE4 long-form population under evaluation is in an activated state reflecting that achieved by PKA phosphorylation. Indeed, we observed (Fig. 2*B*) that the S126D-PDE4D5 mutant, which reflects a population of constitutively activated enzyme (19, 30), exhibits a near-complete ablation to pharmacological activation by challenge with MR-L2 (additional in *SI Appendix*, Fig. S2*D*)

MAPKAPK2 (MK2) also phosphorylates PDE4 long forms in UCR1, but at a different site (Ser133 of PDE4D5; Fig. 2*A*; ref.

18) from that at which PKA acts. Instead of activation, MK2 phosphorylation serves to attenuate the level of activation elicited by PKA phosphorylation. We therefore investigated whether the activity of MR-L2 could be influenced by MK2 phosphorylation using an engineered MK2 phosphomimetic mutant (S133D-PDE4D5) that is known to mimic effectively the MK2-phosphorylated protein state (18). We noted that the S133D-PDE4D5 mutant, when examined in isolation, was activated by MR-L2 to a similar extent to wild-type PDE4D5 (Fig. 2*C*). Interestingly, while the PKA-phosphomimicking S126D-PDE4D5 mutant was insensitive to pharmacological activation by MR-L2 (Fig. 2*B*), the addition of a MK2 phosphomimetic mutation alongside the phosphomimetic PKA mutation (S126D:S133D-PDE4D5) acted to partially restore sensitivity of the PKA phosphomimetic mutant of PDE4D5 to pharmacological activation by MR-L2 (Fig. 2*C*). This demonstrates that additional posttranslational modification of long PDE4 isoforms can influence the pharmacological activation elicited by MR-L2, including where prior PKA mediated phosphorylation and activation of long-form PDE4 enzymes is present. In this instance, it seems likely that MR-L2 acts to overcome the attenuating effect that MK2 phosphorylation exerts on PKA activation of PDE4 long isoforms.

The growth-promoting kinase Erk is able to phosphorylate a serine at the C-terminal end of the conserved PDE4 core catalytic domain of isoforms of PDE4B, PDE4C, and PDE4D, but not PDE4A forms (34). In the case of PDE4 long isoforms, phosphorylation by Erk leads to a reduction in PDE4 catalytic activity that can be restored to basal levels by subsequent PKA-mediated UCR1 phosphorylation, thereby providing a feedback regulatory route in cells (32, 35). The Erk-inhibited state can be mimicked by the cognate Ser:Asp mutation, as exemplified previously with the Ser651Asp-PDE4D5 mutant (Fig. 2*A*) (32). In a manner that parallels the action of endogenous PKA phosphorylation (32), we show here that MR-L2 challenge of Ser651Asp-PDE4D5 leads to a comparable increase in activity to that seen when employing wild-type PDE4D5 (Fig. 2*D*). Thus, treatment with the MR-L2 activator compound phenocopies the action of PKA phosphorylation in overcoming the ERK-mediated inhibition of PDE4 long-isoform activity.

Activation by MR-L2 Requires the Dimeric Assembly of Long-Form PDE4D5. PDE4 long isoforms form dimers (23, 36), and such organization is essential for their autoinhibitory regulation by the UCR modules and for their activation subsequent to PKA-mediated phosphorylation (36). Dimerization involves two pivotal binding interfaces. One of these is located in the PDE4 catalytic unit, while the other involves the long-form UCR1 module forming a four-helix bundle assembly with UCR2 in the dimer (23, 37–39). Together, these interfaces confer an architecture that allows autoinhibitory cross-capping (40) of the catalytic pocket by UCR2 so as to gate substrate entry. Simultaneous disruption of both dimerization interfaces destroys the ability of full-length PDE4 long isoforms to dimerize and results in the formation of long-form monomers that, as with monomeric short forms, are catalytically active (23). Long-form monomers can be engineered by mutations at two discrete loci: namely triple alanine mutation of an Arg:Asn:Asn motif (173-RNN-175 in PDE4D5) in the UCR1-located dimerization interface combined with a single Arg-to-Asp charge reversal mutation at the catalytic domain interface (R499 in PDE4D5) (23). We have previously shown (23) that the monomeric Arg173Ala:Asn174Ala:Asn175Ala:Arg499Asp-PDE4D5 mutant ("DD1-R499D-PDE4D5") lacks sensitivity to activation by PKA, consistent with dismantling of the quaternary structure organization that underpins regulatory cross-capping of the cAMP substrate binding sites in the functional dimers. Here, we demonstrate a parallel effect with the pharmacological activation of PDE4D5, where the monomeric DD1-R499D-PDE4D5 mutant showed complete loss of sensitivity to activation by MR-L2 (Fig. 2*E*). This suggests that the mechanism of action of MR-L2, as with PKA phosphorylation of long PDE4 isoforms, involves modulation of autoinhibitory UCR2 cross-capping within the PDE4 long-form dimeric assembly.

MR-L2 Elicits an Allosteric Activation of the PDE4D5 Long Isoform. As PKA phosphorylation increases the V_{max} for cAMP hydrolysis of PDE4 long isoforms without affecting the K_m for cAMP (19, 30, 31), we set out to determine the kinetics of MR-L2 action on cAMP hydrolysis by PDE4D5. Indeed, MR-L2 acts as a reversible, noncompetitive activator of PDE4D5 (Fig. 2 *F* and *G*), displaying an increase in the apparent V_{max} for cAMP hydrolysis without affecting the apparent K_m for cAMP. Such kinetic data are consistent with MR-L2 binding to an allosteric regulatory site on PDE4 long isoforms to exert its stimulatory action.

The Pharmacological Activation of Long PDE4 Isoforms Lowers Intracellular cAMP in Madin–Darby Canine Kidney Cells. ADPKD is characterized by the formation and expansion of multiple cystic structures arising from the tubular segments of the nephron. The genetic abrogation of either polycystin-1 (PKD1) or polycystin-2 (PKD2) leads to diminished intracellular Ca^{2+} levels and, thereby, the chronic activation of Ca^{2+}-inhibited adenylyl cyclase-5/6. This results in abnormally elevated cAMP levels that drive proliferative signaling and enhanced fluid transport, resulting in the formation, expansion, and swelling of multiple cystic structures within the kidney (25, 26, 41). Madin–Darby canine kidney (MDCK) cells maintain the normal integrity of epithelial cell polarity and adherens junctions, and can be triggered to form cysts (cystogenesis) upon chronic stimulation of adenylyl cyclase, providing a cellular model for cAMP-dependent cyst formation in ADPKD (24, 25, 42). MDCK cells express PDE4C and PDE4D long-form variants as well as PDE4A and PDE4B short isoforms, and their expression was unaffected by incubation with MR-L2 (Fig. 3*A* and *SI Appendix*, Fig. S2*E*). Upon challenging MDCK cells with forskolin (3 μM; 15 min), a direct activator of adenylyl cyclase, we found that cells that had been pretreated with MR-L2 exhibited significantly suppressed cAMP elevation (Fig. 3*B*). These results were further supported by cAMP-responsive fluorescence resonance energy transfer (FRET) experiments, conducted in HEK293 cells, where MR-L2 suppressed the baseline-normalized cAMP FRET response to forskolin (1 μM) (*SI Appendix*, Fig. S3*A*).

To confirm that the suppression of cAMP was due to the pharmacologically enhanced activity of long-form PDE4 enzymes, we then conducted a series of assays in the presence of the PDE4-specific inhibitor, roflumilast (100 nM). We hypothesized that inhibition of PDE4 activity, through occupancy of the catalytic site by the PDE4 inhibitor, would ablate the suppression of cAMP accumulation by inactivating the catalytic activity of the PDE4 long-form target of the allosteric activator. Indeed, we found that, in MDCK cells, the inhibition of PDE4 activity, by a saturating concentration of roflumilast (100 nM), ablated the suppressive effect of MR-L2 (3 μM), thereby confirming that the catalytic activity of PDE4 is required for the action of MR-L2 (Fig. 3*C*).

Interestingly, cAMP is known to be excreted from the kidney epithelia (see, e.g., ref. 43). For that reason, we investigated whether the MR-L2–mediated reduction in intracellular cAMP could be due to enhanced excretion from the MDCK cells. Thus, we assessed the extracellular cAMP levels after forskolin (3 μM) treatment of cells, with and without MR-L2 (3 μM) pretreatment. We found that, in parallel to the MR-L2–elicited suppression of intracellular cAMP levels, the extracellular level of cAMP was also significantly reduced by MR-L2 treatment (Fig. 3*D*). This demonstrates that cAMP excretion is not enhanced by MR-L2 treatment and that reducing intracellular cAMP levels, consequentially, leads to decreased cAMP export.

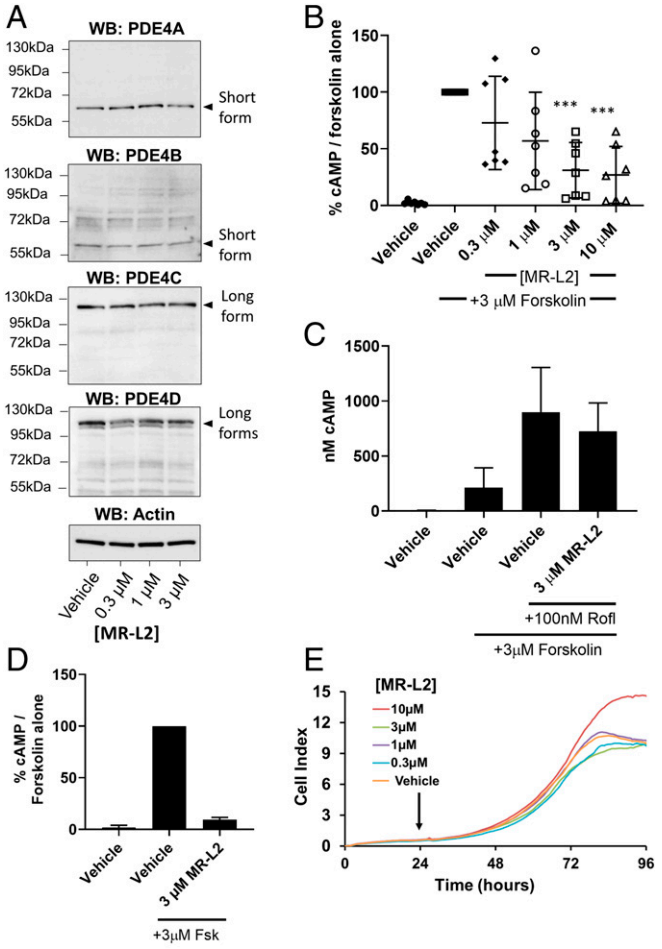

Fig. 3. MR-L2 reduces intracellular cAMP in MDCK cells without affecting PDE4 expression or cell viability. (*A*) MDCK cells were grown in 2D culture and treated with increasing concentrations of MR-L2. Western blot analysis of protein extracts shows the expression of short-form PDE4A and PDE4B and PDE4D, as well as long forms of PDE4C and PDE4D. Based upon their observed gel migration and predicted molecular weights, these bands are likely to represent PDE4A1, PDE4B2, PDE4C1/3, PDE4D1/2, PDE4D5/7, and PDE4D3/8/9 (in some cases, multiple isoform variants comigrate due to similar molecular weights). The expression of these isoform variants was not affected by 1-h incubation with MR-L2. β-Actin was used as a protein loading control. Quantitation of multiple Western blot analysis is presented in *SI Appendix*, Fig. S2*E*. (*B*) A 1-h pretreatment with MR-L2 suppresses cAMP accumulation in response to acute treatment with 3 μM forskolin (15 min). Mean of $n = 7$ independent experiments (±SD). Data points represent independent experimental results. (*C*) The suppressive effects of 1-h pretreatment with 3 μM MR-L2 on forskolin (3 μM, 15 min)-stimulated cAMP accumulation was ablated by cotreatment with the PDE4 inhibitor roflumilast (100 nM). Results show the mean of three independent experiments, and error bars represent SD. (*D*) Extracellular cAMP was assessed in response to MR-L2 (3 μM) incubation for 1 h before forskolin (3 μM, 15 min) challenge. Extracellular cAMP accumulation was reduced in the MR-L2 samples, indicating that the intracellular reduction in global cAMP was not due to enhanced excretion from the cell. Data from three independent experiments are shown. (*E*) MR-L2 treatment exhibited no deleterious effects on the proliferation of MDCK cells in 2D culture using the xCELLigence impedance-based assay system. MR-L2 was added to the culture 24 h after inception of the assay.

We confirmed that the activator compounds were not acting as cytotoxic agents in these 2D culture assays using the xCELLigence electrical-impedance–based assay system (Fig. 3*E*). The expected exponential growth rate was observed for untreated cells, and there was no effect of MR-L2 on cell number, demonstrating a lack of overt cytotoxicity.

The Pharmacological Activation of Long PDE4 Isoforms Suppresses MDCK Cyst Formation. Using the MDCK cell line as a model for kidney cyst formation in 3D culture (24, 25, 42), we then interrogated whether PDE4 activity can modulate cAMP-mediated cyst expansion using the archetypal PDE4 inhibitor rolipram. We found that the inhibition of PDE4 exacerbates agonist-driven cyst formation in a concentration-dependent manner (Fig. 4*A*). In this regard, it is possible that pan-PDE4 inhibitors used clinically (7, 13, 14) may adversely exacerbate cyst formation in individuals either suffering from ADPKD or harboring mutations that may lead to the clinical manifestations of ADPKD.

Having established that modulation of PDE4 activity regulates the cAMP-mediated cystic response, we then tested whether amplifying PDE4-mediated cAMP degradation, using MR-L2, could suppress the cystic phenotype. We evaluated this in cells challenged with a fixed concentration of PGE2 (300 nM), observing a concentration-dependent suppression of cyst formation by MR-L2 (Fig. 4 *B* and *C*), with an EC_{50} of 1 μM. Interestingly, in the cellular context, we found that the potency of MR-L2 was higher than in the biochemical PDE4D5 enzyme activation assay. Such enhanced cellular potency was seen in both the cAMP assay and the cyst formation assay. This suggests that the functional long-form PDE4 target in these cells has an enhanced sensitivity to MR-L2 compared with the ectopically expressed PDE4 long isoforms in HEK293 cells, which may be due to cell type-conferred differences in the conformation and/or posttranslational modification status of the PDE4 long isoform. Indeed, there is a large literature showing that PDE4 isoforms can show dramatically different sensitivities to selective inhibitors dependent upon cellular context (see, e.g., refs. 44–49). Such dramatic differences are thought to be due to altered conformational changes in PDE4 that may be triggered when PDE4 isoforms either interact with certain partner proteins or are subject to specific types of posttranslational modification. Examples of this are provided by, for example, the PKA-mediated phosphorylation of PDE4D3 and the interaction of human PDE4A species with various SH3 domain-containing proteins (9, 13, 22, 30, 50, 51).

To establish that the elevated catalytic activity PDE4 long isoforms elicited by MR-L2 is required to suppress cyst formation, we investigated whether cotreatment with the potent PDE4 inhibitor roflumilast (100 nM) was sufficient to ablate the functionality of MR-L2 by inhibiting the catalytic activity of its PDE4 target. We observed that treatment with roflumilast did, indeed, interdict the suppression of cystogenesis elicited by the pharmacological PDE4 activator MR-L2 (3 μM, Fig. 4*D*).

ATP levels have previously been connected with cyst formation and expansion in the MDCK cell model (52). We therefore set out to determine whether downstream modulation of ATP signaling, in response to long-form PDE4 activation, may contribute to the suppression of cyst formation. We assessed this by measuring the abundance of DNA-normalized ATP levels in whole-well cystic cultures, where we observed a slight reduction (15.6 ± 30% SD) in the ATP/DNA ratio when cells were grown in the presence of MR-L2 (3 μM; Fig. 4*E*).

The differential expression and activity of adenylyl cyclase isoforms has been shown to occur in ADPKD (53, 54), and the AC3, AC5, and AC6 isoforms are expressed in MDCK cells (53, 54). To investigate whether the suppression of cAMP-driven cystogenesis was independent of the mode of activation of adenylyl cyclase, we evaluated a single, nonmaximally effective, concentration of MR-L2 (3 μM) against either (*i*) incremental increases in forskolin concentration (Fig. 5*A*), to drive cystogenesis by direct activation of adenylyl cyclase, or (*ii*) PGE2 stimulation (Fig. 5*B*), to evaluate cystogenesis driven by the G_s-coupled receptor-promoted activation of adenylyl cyclase. The activator, MR-L2, clearly suppressed the maximal cyst response elicited by both such direct and indirect activation of adenylyl cyclase.

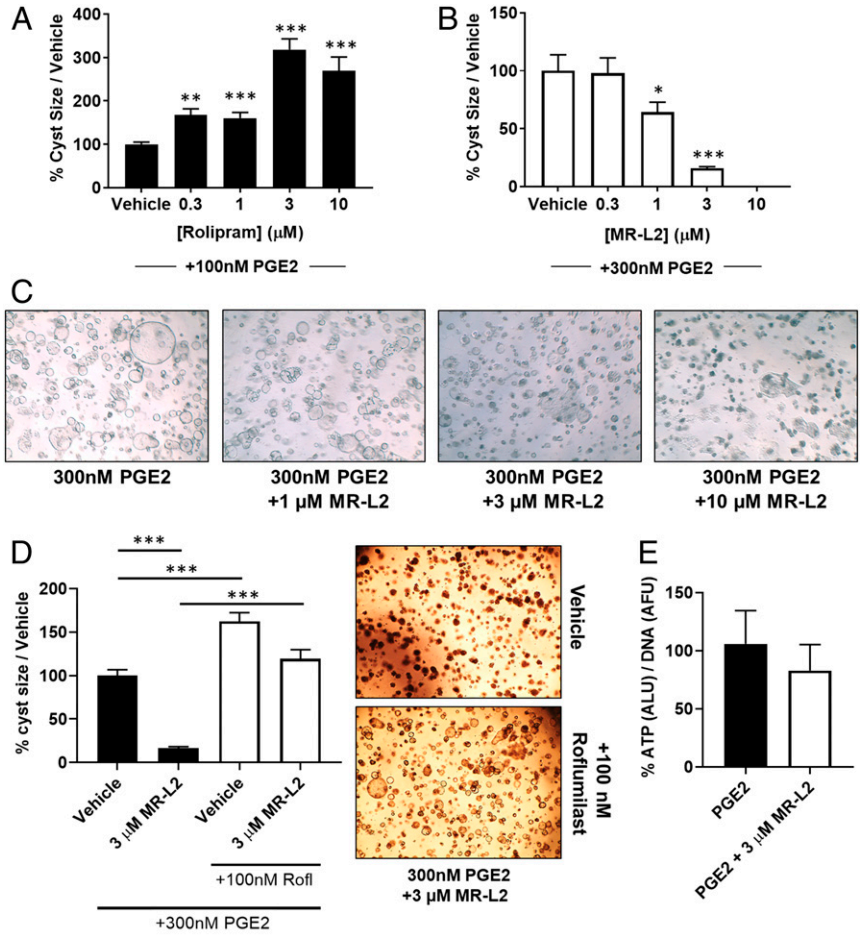

Fig. 4. MDCK cyst formation is regulated by PDE4 activity and is suppressed by pharmacological activation of PDE4 long isoforms. (*A*) MDCK cells were grown in a 3D collagen matrix and treated with increasing concentrations of the PDE4-selective inhibitor, rolipram. Rolipram exacerbates the PGE2-induced formation of large cystic structures, demonstrating that PDE4 enzymes are localized within compartments that control cyst expansion. (*B*) PGE2-induced MDCK cell cyst formation was suppressed by MR-L2 (EC_{50}, 1.2 μM). Data are displayed as a percentage of PGE2 stimulation alone, and error bars represent the SEM of all cysts measured in each condition. (*C*) Representative images of MDCK cysts treated with increasing concentrations of MR-L2. The images illustrate a concentration-dependent suppression of cyst size. (*D*) Cotreatment of PGE2 (300 nM)-stimulated MDCK cystic cultures with roflumilast (100 nM) and/or MR-L2 (3 μM) shows that inhibition of PDE4 catalytic activity ablates the suppressive effects of MR-L2 on cyst growth. Error bars represent the SEM. Representative images of MR-L2, and roflumilast/MR-L2–treated cultures are shown. (*E*) DNA normalized ATP concentrations within the cystic cultures were used as a measurement ATP in the cystic cultures. The balance of ATP signaling in the cystic cultures was not perturbed by MR-L2 treatment.

Activation of PDE4 Long Isoforms Suppresses cAMP-Dependent Cystic Fibrosis Transmembrane Receptor Activation. The cystic fibrosis transmembrane receptor (CFTR) chloride channel is expressed in many tissues including kidney epithelia (55). In response to elevated cAMP, PKA phosphorylates the CFTR at multiple intracellular residues, resulting in channel activation and chloride transport (55). PDE4D long isoforms localize with the CFTR signaling complex and regulate channel activity by lowering local cAMP levels and, thereby, associated PKA activity (56, 57). In ADPKD, activated CFTR facilitates fluid transport into the cystic lumen (55).

MDCK cells retain expression of CFTR, and the role of this ion channel in cyst expansion in this model is well recognized (24, 25, 42, 58, 59). We investigated whether increased cAMP hydrolysis, induced by MR-L2, could suppress CFTR activation in MDCK cells using a membrane depolarization (60). We found that PGE2 treatment depolarized MDCK cell membrane potential in a concentration-dependent manner (Fig. 5*C*) and this was reversed by the addition of a selective CFTR inhibitor ($CFTR_{INH172}$, 100 μM) (*SI Appendix*, Fig. S3*B*). Interestingly, PGE2-elicited CFTR activity was clearly suppressed in a concentration-dependent manner upon MR-L2 pretreatment (Fig. 5*D*). Interestingly, the dose dependency of MR-L2, for both inhibition of MDCK cystogenesis and CFTR depolarization, was near identical when employing PGE stimulation, at either 300 or 100 nM (Fig. 5 *E* and *F*, respectively).

PDE4 Activation Suppresses Cyst Formation in Human Cell Models of ADPKD. We further studied the action of MR-L2 in human models of ADPKD by first profiling the PDE4 isoform composition in four normal (CL5, CL8, CL11, and RFH), and four ADPKD patient-derived cell lines (SKI-001, SKI-002, OX938, and OX161) (42, 61) (*SI Appendix*, Fig. S3*C*). We found that long PDE4B1, PDE4B3, PDE4C3, PDE4D5, PDE4D7, and PDE4D9 isoform as well as short PDE4B2 and PDE4D1/PDE4D2 isoform transcripts were expressed in these cells. Of these transcripts, we found that those for long PDE4D5 and for short PDE4D1/2 were up-regulated in ADPKD cells (*SI Appendix*, Fig. S3*C*). This is consistent with the elevated levels of cAMP driving increased gene expression by virtue of functional CRE motifs known to be located within the promoter elements of their genes (62, 63). Interestingly, we observed the expression of long PDE4C species in the MDCK cell model (Fig. 3*A*) and detected an elevated mRNA expression in two of the human ADPKD mRNA samples. PDE4C exhibits a very restricted expression pattern compared with other PDE4 subfamilies, but it has been connected with the regulation of a PC-2/AKAP150/PKA localized signalosome in the primary cilia and, furthermore, the regulation of PDE4C isoforms by HNF-1 has been linked to ADPKD (64).

We selected one of these immortalized ADPKD kidney cell lines to examine the action of MR-L2 in a cellular context. The immortalized OX161 line was first isolated from a patient with ADPKD who expressed a truncated, nonfunctional form of polycystin-1 (PC1) (42). As with MDCK cells, OX161 cells are responsive to agonists of cAMP signaling, such as forskolin and PGE2, which drive the formation of small cystic structures when cells are grown in a 3D matrix (42). As with the MDCK cell model, we found that, in OX161 cells, cystogenesis is enhanced upon challenge with the PDE4 inhibitor, rolipram (Fig. 6*A*), highlighting the fact that PDE4 activity serves to regulate cystic

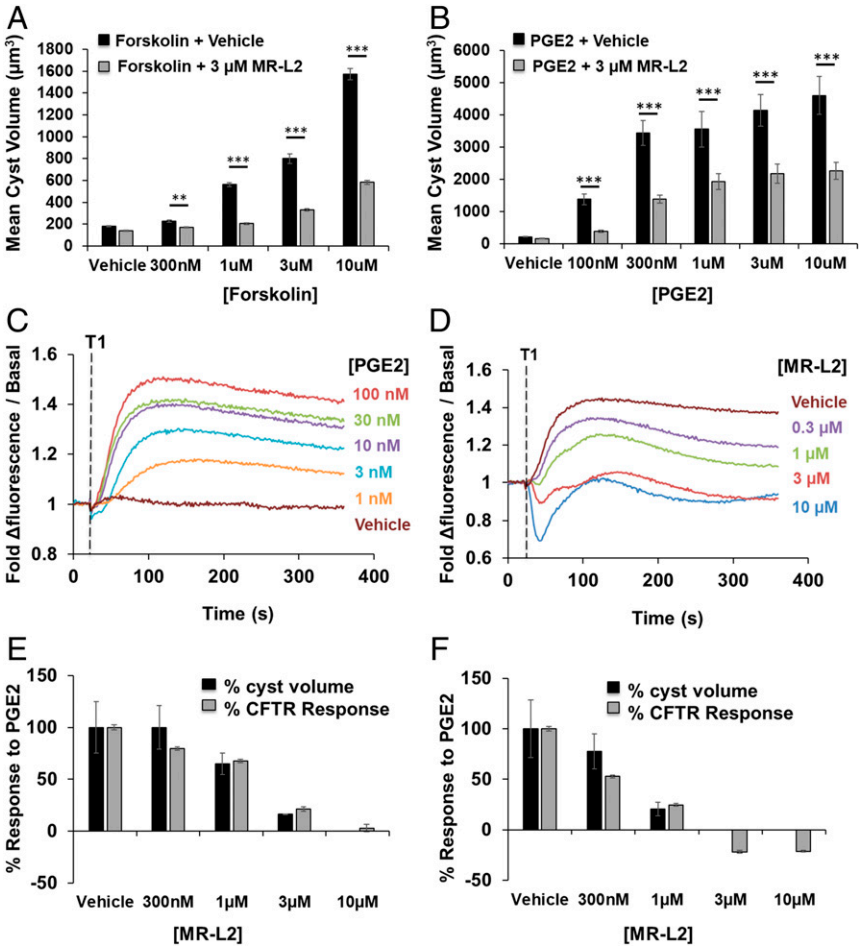

Fig. 5. MR-L2 treatment-mediated MDCK cyst suppression is independent of agonist drive and suppresses PGE2-mediated CFTR activation and membrane depolarization. (*A*) Forskolin treatment drives cyst formation and expansion in a concentration-dependent manner. Activator compound MR-L2 (3 μM) suppressed forskolin-induced cyst formation. Data are displayed as mean ± SEM of all cysts measured in each experimental condition. (*B*) PGE2-stimulated MDCK cyst formation was also suppressed by PDE4 long-form activation with 3 μM MR-L2. Data are displayed as mean ± SEM of all cysts measured in each experimental condition. (*C*) MDCK cells exhibit a concentration-dependent membrane depolarization in response to PGE2-mediated CFTR activation using a fluorescent dye-based assay for membrane potential. Individual fluorescence traces over time are shown for each PGE2 concentration. T1 highlights the time point at which PGE2 was added. (*D*) Cells were preincubated (40 min) with concentrations of the PDE4 long-form activator compound MR-L2, and then challenged with 100 nM PGE2. Increasing concentrations of MR-L2 suppress the PGE2-stimulated increase in fluorescence, indicating that activation of PDE4 is sufficient to dampen the cAMP-driven activation of the CFTR. (*E* and *F*) Cyst assays were conducted in parallel with CFTR assessment. When MDCK cells are stimulated to form cysts with either 300 nM PGE2 (*E*) or 100 nM PGE2 (*F*), the resulting concentration-dependent suppression of cystic expansion by MR-L2 (black bars, shown as percentage of PGE2 alone; error bars are SEM of all cysts measured in each treatment) closely follows the down-regulation of CFTR-mediated membrane depolarization (gray bars, fold change in fluorescence).

potential of human ADPKD cells. Similar to what we observed with MDCK cells, we found that MR-L2 attenuated the PGE2-stimulated cystogenesis of OX161 cells (Fig. 6*B*).

PDE4 Activation Suppresses Cyst Formation in Primary Cultures of ADPKD Patient-Derived Kidney Epithelial Cells. We then went on to assess the functionality of MR-L2 in primary human cell cultures that were collected from the cysts of an ADPKD patient's kidney. Such cells form fluid-filled cysts in 3D culture and are responsive to stimuli that increase cAMP, such as forskolin (*SI Appendix*, Fig. S4*A*) and PGE2 (*SI Appendix*, Fig. S4*B*). Interestingly, while immortalized culture models such as OX161 cells fail to respond to vasopressin, an important accentuator of cyst formation, these primary cells were found to be vasopressin-sensitive (*SI Appendix*, Fig. S4*C*), thus mirroring the pathological situation in vivo. It must be noted, however, that at the concentrations of AVP tested, this G_s-coupled receptor agonist elicited a lower level of stimulation than did the G_s-coupled receptor agonist PGE2. This may reflect cAMP compartmentalization such that these receptors activate distinct pools of adenylyl cyclases, showing not only different degrees of activation but also different spatial localization within the plasma membrane conferring distinct cellular functionalities and potential for being differentially regulated by distinct long-form PDE4 populations. Consistent with their origins in diseased kidney tissue, these primary cell cultures spontaneously form large cystic structures in vitro (Fig. 6*C*). Furthermore, MR-L2 clearly suppressed the number of cysts formed in 3D culture in both unstimulated (Fig. 6*C*) and vasopressin-treated (10 nM) cell cultures (Fig. 6*D*) without adversely affecting cell viability (Fig. 6 *E*–*G*).

Discussion

PDE4 family isoforms are ubiquitously expressed and play a fundamental role in determining the spatial compartmentalization of cAMP signaling in cells. They also act as nodes for conferring cross talk via inputs from various other signaling pathways through multisite phosphorylation (8, 10, 12, 13, 29). Furthermore, long PDE4 isoforms play a key role in determining cellular desensitization to cAMP signaling through a feedback loop involving their PKA-mediated phosphorylation and activation (17, 18, 65). This process is restricted to long PDE4 isoforms, as PKA phosphorylates a serine residue located within UCR1 (a regulatory module conserved across long isoforms from all PDE4 subfamilies) but that is absent from PDE4 short and super-short forms and is not found in any other PDE family (19, 30, 31). The adjacent UCR2 region, although found in all PDE4 isoforms (whether long or short), exerts an autoinhibitory action that is specific to the long forms and serves to diminish, but does not fully abolish, their catalytic activity (37). The mechanistic basis for this arises from the interaction of UCR2 with UCR1. Thus, together, UCR2 and UCR1 interact to form a combined regulatory module (66) that docks over the catalytic pocket (38). This UCR1/2 module imposes a constraint on long-form PDE4 catalytic activity that is ablated by PKA phosphorylation of UCR1, leading to an increase in activity of, typically, some 40–80% (19, 22, 29, 37, 38). Given the high catalytic turnover of PDE4, this degree of activation has the ability to generate a profound decrease in cAMP levels in cells, thereby regulating cAMP-responsive processes (17–19, 65).

Here, we describe the discovery of a long-form PDE4-activating ligand, namely, the *N*-substituted-2-(3-aryl-1*H*-1,2,4-triazol-1-yl)acetamide chemotype of MR-L2 (Fig. 1*A*). It acts to

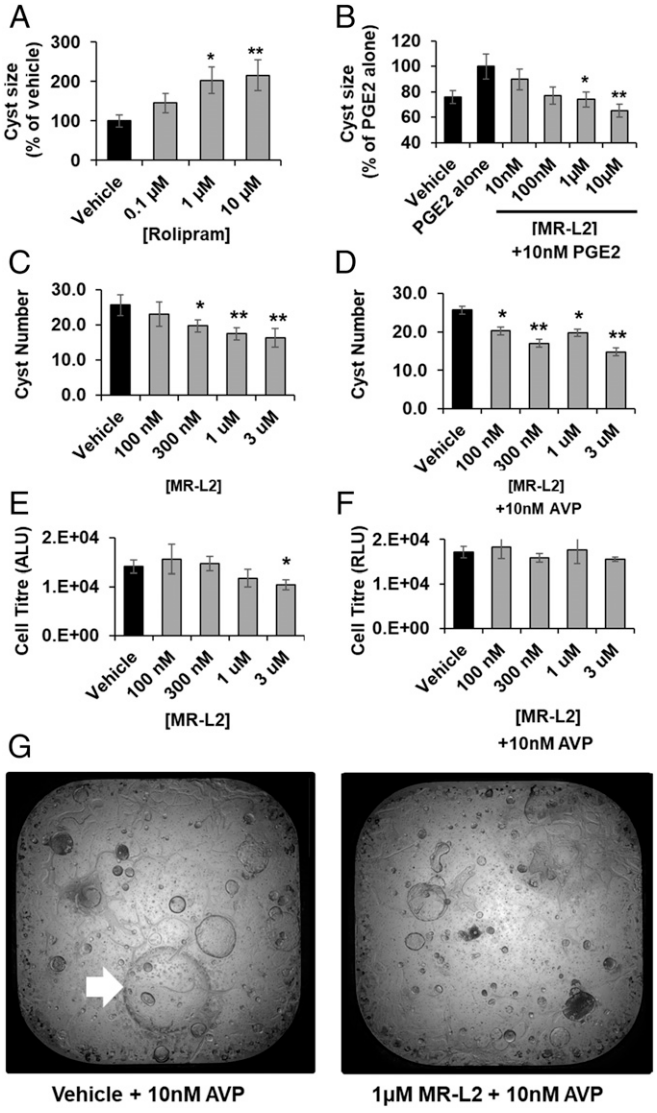

Fig. 6. MR-L2 inhibits cyst formation in human models of ADPKD. (*A*) Treatment with the PDE4-selective inhibitor, rolipram, exacerbates the expansion of cysts formed by the OX161 cell line when grown in 3D culture. Data are expressed as a percentage of vehicle [0.1% (vol/vol) DMSO] control treatment and displayed as mean ± SEM of all cysts measured in each condition. (*B*) MR-L2 suppresses the formation of PGE2-stimulated OX161 cell cysts in a concentration-dependent manner. Mean cyst size is shown as a percentage of the PGE2-alone treatment group, where MR-L2 reduces mean cyst size to below unstimulated [0.1% (vol/vol) DMSO] levels. (*C*) Primary human cells from a patient with ADPKD were cultured from single kidney cysts. MR-L2 suppresses the spontaneous cyst formation of diseased primary human kidney epithelial cells. Cyst number decreases in response to MR-L2 treatment. Error bars represent the SD of four treatments. (*D*) MR-L2 suppresses the vasopressin-exacerbated, ADPKD-driven, cyst formation of diseased primary human kidney epithelial cells. Cyst number decreases in response to MR-L2 treatment. Error bars represent the SD of four treatments. (*E* and *F*) Primary human ADPKD cell viability was not adversely affected by MR-L2 treatment, as assessed using a luminescence-based detection of ATP as a function of living cells. Data are displayed in relative luminescence units, with error bars representing the SD of four treatments. (*G*) Composite confocal microscopy of primary human cystic cultures under treatment with 10 nM vasopressin and concentrations of MR-L2. Cystic structures are seen as spherical, lumen-forming, cellular outgrowths. Epithelial tubules and supporting cellular matrices are also present within the cultures but are not overtly affected by the presence of MR-L2 (additional imaging available in *SI Appendix*, Fig. S4).

phenocopy the stimulatory effect exerted by PKA phosphorylation on dimeric PDE4 long isoforms (19, 31, 35, 37). Thus, we have shown that the stimulatory effect of MR-L2 (*i*) is restricted to PDE4 family enzymes and specific to long-form variants; (*ii*) that it is not additive with the stimulatory effect of PKA on long isoforms; (*iii*) that it requires the dimeric state that is adopted by long, but not short, PDE4 isoforms; (*iv*) that it is operative on PDE4 long isoforms showing attenuated activity due to phosphorylation by Erk MAP kinase; and (*v*) that it elicits comparable levels of activation to those caused by PKA-mediated phosphorylation of PDE4 long isoforms.

The action of MR-L2 is reversible and exhibits kinetics of noncompetitive activation. These data are consistent with the compounds binding to an allosteric site on the enzyme. We propose that, as has been suggested for PKA phosphorylation-mediated activation, this drives an equilibrium shift away from a UCR1/UCR2-capped autoinhibited conformational state toward disinhibited conformational state(s) (29, 37, 38). It is known that UCR1 engages with UCR2 directly to form a tandem regulatory module (66). Insight into a mechanism whereby the UCR1/UCR2 module might regulate catalytic activity has been gauged from crystal structures showing that a helix within UCR2 can fold across the entrance to the catalytic pocket to gate substrate entry (67). Although complete structural characterization of full-length PDE4 species remains elusive, further advances with crystallographic studies (40) have now unambiguously confirmed hypotheses (40, 68) that UCR2 gating of the catalytic pocket involves cross-capping within the dimeric long-form PDE4 structures. Thus, regulatory control of long-form PDE4 activity requires the enzyme to be in a dimeric configuration with alterations in activity likely mediated by modulation of the equilibrium position between the UCR2-capped and -uncapped states, thereby exerting V_{max} kinetic control over cAMP hydrolysis. Presumably, such a transition leading to uncapping and increased catalytic activity can be triggered either natively, when PKA phosphorylates UCR1, or pharmacologically, when a small-molecule activator binds to its allosteric site.

As with PKA phosphorylation (17–19, 30), we show that the prototypical allosteric activator, MR-L2, can decrease intracellular cAMP levels in cells where long PDE4 isoforms are expressed. Moreover, it is expected that the observed reduction in global cAMP concentration will not be homogenously distributed throughout the cell, and that effects may be more pronounced at key nanodomain signaling complexes. At such sites in intact cells, the protein complexation and or posttranslational modification status of target PDE4 species may give rise to altered sensitivity to activator compounds relative to that seen in our biochemical enzyme assay based on cell lysates. Such compounds might have therapeutic potential in diseases where chronic cAMP elevation provides the underpinning molecular pathology. One such disease is ADPKD (21, 26, 41, 69). This is a genetically defined disease that is underpinned by mutations in *PKD1* or *PKD2*, leading to loss or diminution of their function. The consequences of this are lowered intracellular Ca^{2+} levels that lead to disinhibition of adenylyl cyclases-5/6 and thence to elevation of cAMP. Such chronically elevated cAMP levels drive the formation and swelling of kidney cysts that, eventually, lead to kidney failure. The variety of PDE4 long isoforms that kidney cells express (70, 71) (Fig. 3*A* and *SI Appendix*, Fig. S3*C*) provide targets for activator compounds such as MR-L2, suggesting a potential therapeutic strategy. Indeed, we show here that not only does MR-L2 decrease intracellular cAMP but that it also attenuates CFTR activity, which is stimulated by cAMP-driven activation of PKA, and cyst formation in the model MDCK cell system. MR-L2 was also successful in suppressing cyst expansion in an immortalized kidney cell line, OX161, derived from an ADPKD patient, and we further show that the compound suppresses the formation of cysts in 3D cultures of primary human kidney epithelial cells isolated from an ADPKD patient.

In summary, MR-L2 pharmacologically activates dimeric PDE4 long-form variants through a mechanism that phenocopies both the magnitude and mechanism of PKA-mediated PDE4 long-isoform activation. This provides a route to evaluate the consequences of specifically activating this group of PDE4 isoforms. Moreover, the discovery and initial characterization of this drug-like PDE4 activator, together with the demonstration that it can inhibit the in vitro formation of kidney cysts that characterize ADPKD, suggests that direct pharmacological activation of PDE4 long forms may have therapeutic utility in diseases driven by chronically up-regulated cAMP levels.

Materials and Methods

Chemicals and Reagents. Unless otherwise specified, reagents were sourced from Sigma-Aldrich. MR-L2 was synthesized as described in patent WO2016151300.

Cell Culture. HEK293 and MDCK (ATCC) cells were cultured in DMEM (Lonza) supplemented with 10% (vol/vol) FBS (Invitrogen). Human primary epithelial cells were sourced from DiscoveryBioMed and cultured in proprietary media supplied by DBM. Transfection into mammalian cells was conducted using the Lipofectamine 3000 reagent (Invitrogen) as per the manufacturer's instruction.

Molecular Biology. pcDNA3.1 (Invitrogen) was used as the standard vector for mammalian expression, and all site-directed mutagenesis was conducted using the QuikChange mutagenesis kit (Agilent Technologies).

cAMP Phosphodiesterase Assay. Cells were collected in KHEM buffer [50 mM KCl, 10 mM EGTA, 50 mM Hepes (pH 7.2), 1.92 mM $MgCl_2$, pH 7.4 with KOH] and lysed by mechanical disruption. Lysate was precleared by centrifugation at 2,000 × *g* for 10 min before centrifugation at 100,000 × *g* for 30 min. The protein concentration of the supernatant was determined by BCA assay (Sigma). The cAMP PDE assays were then conducted as previously described, using protein concentrations (typically 200 ng to 1 μg per reaction) and incubation times (10 min) that yielded linear rates of reaction as described before by us (72).

Western Blot. Cells were lysed for 20 min in a whole-cell lysis buffer [1% (vol/vol) Triton X-100, 25 mM Hepes, 2.5 mM EDTA, 150 mM NaCl, 50 mM NaF, and 30 mM NaPPi] containing a protease inhibitor mixture (Roche). Insoluble material was removed by centrifuge at 14,000 × *g*. Protein concentration was measured by standard BCA assay (Sigma) before the addition of SDS sample buffer (Invitrogen). The antisera raised against PDE4 have previously been described (19, 73).

cAMP ELISA. Assays were conducted using a cAMP ELISA kit (Enzo) following the manufacturer's instructions and using pre-prepared reagents supplied by the manufacturer.

MDCK Cyst Assay. Collagen type I from rat tail (Invitrogen) was used to form the 3D matrix for culture of MDCK cystic organoids. The assays were conducted in 24- or 96-well plate format with a final concentration of 1 mg/mL collagen matrix. Images were captured using a Motic phase contrast microscope set at 4× magnification. Cystic diameter was recorded, from which cyst volume (V) was calculated using the formula $V = 4/3\ \pi\ r^3$, where r is the radius of the cyst. Typically, between 100 and 300 cysts were measured in each treatment condition, expressed as mean cystic volume ± SEM. DNA normalized ATP levels were measured upon completed of cyst assays where DNA was first labeled using 20 μM Hoechst for 1 h at 37 °C and quantified by fluorescence measurement at 361–486 nm. ATP levels were then assessed using CellTiter-Glo 3D reagent (Promega).

xCELLigence Assays. Assays were conducted as previously described (74). MDCK cells were plated at a density of 5,000 cells per well and allowed to adhere for 24 h before treatment.

OX161 Cyst Assay. OX161 cells were cultured, and assays were conducted as previously described (42, 61).

Primary Human Kidney Cell Cyst Assay. Single-cyst–derived or tissue-derived primary cultures were derived from kidney tissue specimens from de-identified human ADPKD patients under Western Institutional Review Board (WIRB) approval. Informed consent was obtained by third-party vendor interchanges (National Disease Research Interchange and American Association of Tissue Banks) that procure remnant human tissue for biomedical research. Primary human ADPKD cells were grown in biogels containing DiscoveryBioMed RenalCyte media. Manual imaging and cyst counting was conducted in 96-well plates, and automated imaging of the entire well of 384-well plates was conducted.

CFTR Assay. MDCK cells were seeded in 96-well clear-bottom assay plates 4 d before inception of the assay. Assays were conducted in low Cl^- buffer [140 mM Na gluconate, 5 mM K gluconate, 10 mM glucose, 10 mM Hepes (free acid), 1 mM $CaCl_2$, 1 mM $MgCl_2$, pH 7.4 with NaOH] supplemented with FLIPR Membrane Potential Assay Kit Blue (Molecular Devices; R8042) and Amiloride (10 μM) (75). Assays were conducted using the Flex Station 3 (Molecular Devices), where real-time measurements of fluorescence were recorded at excitation 530 nm and emission 565 nm.

Statistical Analysis. Pairwise comparison of data was conducted by *t* test, or Mann–Whitney test. One-way ANOVA with Dunnett's multiple-comparison test was conducted where multiple comparisons within the data were made. Statistical significance is annotated as follows: $^{***}P \leq 0.001$, $^{**}P \leq 0.01$, and $^{*}P \leq 0.05$.

ACKNOWLEDGMENTS. A.C.M.O. and M.L. acknowledge research support from Kidney Research United Kingdom (Grant RP40/2014). E.K. acknowledges research support from Bundesministerium für Bildung und Forschung (16GW0179K), Deutsche Forschungsgemeinschaft (KL1415/7-1 and 394046635–SFB 1365), and the German–Israeli Foundation (I-1452-203/13-2018).

1. K. Taskén, E. M. Aandahl, Localized effects of cAMP mediated by distinct routes of protein kinase A. *Physiol. Rev.* **84**, 137–167 (2004).
2. E. Parnell, T. M. Palmer, S. J. Yarwood, The future of EPAC-targeted therapies: Agonism versus antagonism. *Trends Pharmacol. Sci.* **36**, 203–214 (2015).
3. M. Schmidt, F. J. Dekker, H. Maarsingh, Exchange protein directly activated by cAMP (epac): A multidomain cAMP mediator in the regulation of diverse biological functions. *Pharmacol. Rev.* **65**, 670–709 (2013).
4. R. F. Schindler, T. Brand, The Popeye domain containing protein family—a novel class of cAMP effectors with important functions in multiple tissues. *Prog. Biophys. Mol. Biol.* **120**, 28–36 (2016).
5. D. H. Maurice *et al*., Advances in targeting cyclic nucleotide phosphodiesterases. *Nat. Rev. Drug Discov.* **13**, 290–314 (2014).
6. T. Keravis, C. Lugnier, Cyclic nucleotide phosphodiesterases (PDE) and peptide motifs. *Curr. Pharm. Des.* **16**, 1114–1125 (2010).
7. S. H. Francis, M. A. Blount, J. D. Corbin, Mammalian cyclic nucleotide phosphodiesterases: Molecular mechanisms and physiological functions. *Physiol. Rev.* **91**, 651–690 (2011).
8. M. D. Houslay, Underpinning compartmentalised cAMP signalling through targeted cAMP breakdown. *Trends Biochem. Sci.* **35**, 91–100 (2010).
9. M. D. Houslay, G. S. Baillie, D. H. Maurice, cAMP-Specific phosphodiesterase-4 enzymes in the cardiovascular system: A molecular toolbox for generating compartmentalized cAMP signaling. *Circ. Res.* **100**, 950–966 (2007).
10. M. Conti *et al*., Cyclic AMP-specific PDE4 phosphodiesterases as critical components of cyclic AMP signaling. *J. Biol. Chem.* **278**, 5493–5496 (2003).
11. A. Lerner, P. M. Epstein, Cyclic nucleotide phosphodiesterases as targets for treatment of haematological malignancies. *Biochem. J.* **393**, 21–41 (2006).
12. M. D. Houslay, PDE4 cAMP-specific phosphodiesterases. *Prog. Nucleic Acid Res. Mol. Biol.* **69**, 249–315 (2001).
13. M. D. Houslay, P. Schafer, K. Y. Zhang, Keynote review: Phosphodiesterase-4 as a therapeutic target. *Drug Discov. Today* **10**, 1503–1519 (2005).
14. C. P. Page, D. Spina, Phosphodiesterase inhibitors in the treatment of inflammatory diseases. *Handb. Exp. Pharmacol.*, 391–414 (2011).
15. S. L. Jin, S. L. Ding, S. C. Lin, Phosphodiesterase 4 and its inhibitors in inflammatory diseases. *Chang Gung Med. J.* **35**, 197–210 (2012).
16. D. Mika, M. Conti, PDE4D phosphorylation: A coincidence detector integrating multiple signaling pathways. *Cell. Signal.* **28**, 719–724 (2016).
17. N. Oki, S. I. Takahashi, H. Hidaka, M. Conti, Short term feedback regulation of cAMP in FRTL-5 thyroid cells. Role of PDE4D3 phosphodiesterase activation. *J. Biol. Chem.* **275**, 10831–10837 (2000).
18. K. F. MacKenzie *et al*., Phosphorylation of cAMP-specific PDE4A5 (phosphodiesterase-4A5) by MK2 (MAPKAPK2) attenuates its activation through protein kinase A phosphorylation. *Biochem. J.* **435**, 755–769 (2011).
19. S. J. MacKenzie *et al*., Long PDE4 cAMP specific phosphodiesterases are activated by protein kinase A-mediated phosphorylation of a single serine residue in upstream conserved region 1 (UCR1). *Br. J. Pharmacol.* **136**, 421–433 (2002).
20. G. Némoz, C. Sette, M. Conti, Selective activation of rolipram-sensitive, cAMP-specific phosphodiesterase isoforms by phosphatidic acid. *Mol. Pharmacol.* **51**, 242–249 (1997).

21. L. Wang *et al*., UCR1C is a novel activator of phosphodiesterase 4 (PDE4) long isoforms and attenuates cardiomyocyte hypertrophy. *Cell. Signal.* **27**, 908–922 (2015).
22. W. Richter, M. Conti, The oligomerization state determines regulatory properties and inhibitor sensitivity of type 4 cAMP-specific phosphodiesterases. *J. Biol. Chem.* **279**, 30338–30348 (2004).
23. G. B. Bolger *et al*., Dimerization of cAMP phosphodiesterase-4 (PDE4) in living cells requires interfaces located in both the UCR1 and catalytic unit domains. *Cell. Signal.* **27**, 756–769 (2015).
24. R. Mangoo-Karim, M. Uchic, C. Lechene, J. J. Grantham, Renal epithelial cyst formation and enlargement in vitro: Dependence on cAMP. *Proc. Natl. Acad. Sci. U.S.A.* **86**, 6007–6011 (1989).
25. D. P. Wallace, Cyclic AMP-mediated cyst expansion. *Biochim. Biophys. Acta* **1812**, 1291–1300 (2011).
26. V. E. Torres, P. C. Harris, Strategies targeting cAMP signaling in the treatment of polycystic kidney disease. *J. Am. Soc. Nephrol.* **25**, 18–32 (2014).
27. A. C. M. Ong, O. Devuyst, B. Knebelmann, G. Walz; ERA-EDTA Working Group for Inherited Kidney Diseases, Autosomal dominant polycystic kidney disease: The changing face of clinical management. *Lancet* **385**, 1993–2002 (2015).
28. A. C. M. Ong, P. C. Harris, A polycystin-centric view of cyst formation and disease: The polycystins revisited. *Kidney Int.* **88**, 699–710 (2015).
29. M. D. Houslay, D. R. Adams, PDE4 cAMP phosphodiesterases: Modular enzymes that orchestrate signalling cross-talk, desensitization and compartmentalization. *Biochem. J.* **370**, 1–18 (2003).
30. R. Hoffmann, I. R. Wilkinson, J. F. McCallum, P. Engels, M. D. Houslay, cAMP-specific phosphodiesterase HSPDE4D3 mutants which mimic activation and changes in rolipram inhibition triggered by protein kinase A phosphorylation of Ser-54: Generation of a molecular model. *Biochem. J.* **333**, 139–149 (1998).
31. C. Sette, M. Conti, Phosphorylation and activation of a cAMP-specific phosphodiesterase by the cAMP-dependent protein kinase. Involvement of serine 54 in the enzyme activation. *J. Biol. Chem.* **271**, 16526–16534 (1996).
32. G. Baillie, S. J. MacKenzie, M. D. Houslay, Phorbol 12-myristate 13-acetate triggers the protein kinase A-mediated phosphorylation and activation of the PDE4D5 cAMP phosphodiesterase in human aortic smooth muscle cells through a route involving extracellular signal regulated kinase (ERK). *Mol. Pharmacol.* **60**, 1100–1111 (2001).
33. F. Naro *et al*., Involvement of type 4 cAMP-phosphodiesterase in the myogenic differentiation of L6 cells. *Mol. Biol. Cell* **10**, 4355–4367 (1999).
34. G. S. Baillie, S. J. MacKenzie, I. McPhee, M. D. Houslay, Sub-family selective actions in the ability of Erk2 MAP kinase to phosphorylate and regulate the activity of PDE4 cyclic AMP-specific phosphodiesterases. *Br. J. Pharmacol.* **131**, 811–819 (2000).
35. R. Hoffmann, G. S. Baillie, S. J. MacKenzie, S. J. Yarwood, M. D. Houslay, The MAP kinase ERK2 inhibits the cyclic AMP-specific phosphodiesterase HSPDE4D3 by phosphorylating it at Ser579. *EMBO J.* **18**, 893–903 (1999).
36. M. Xie *et al*., The upstream conserved regions (UCRs) mediate homo- and hetero-oligomerization of type 4 cyclic nucleotide phosphodiesterases (PDE4s). *Biochem. J.* **459**, 539–550 (2014).
37. W. Richter, M. Conti, Dimerization of the type 4 cAMP-specific phosphodiesterases is mediated by the upstream conserved regions (UCRs). *J. Biol. Chem.* **277**, 40212–40221 (2002).
38. P. Cedervall, A. Aulabaugh, K. F. Geoghegan, T. J. McLellan, J. Pandit, Engineered stabilization and structural analysis of the autoinhibited conformation of PDE4. *Proc. Natl. Acad. Sci. U.S.A.* **112**, E1414–E1422 (2015).
39. M. E. Lee, J. Markowitz, J. O. Lee, H. Lee, Crystal structure of phosphodiesterase 4D and inhibitor complex(1). *FEBS Lett.* **530**, 53–58 (2002).
40. M. D. Houslay, D. R. Adams, Putting the lid on phosphodiesterase 4. *Nat. Biotechnol.* **28**, 38–40 (2010).
41. F. T. Chebib, C. R. Sussman, X. Wang, P. C. Harris, V. E. Torres, Vasopressin and disruption of calcium signalling in polycystic kidney disease. *Nat. Rev. Nephrol.* **11**, 451–464 (2015).
42. E. Parker *et al*., Hyperproliferation of PKD1 cystic cells is induced by insulin-like growth factor-1 activation of the Ras/Raf signalling system. *Kidney Int.* **72**, 157–165 (2007).
43. R. A. M. H. van Aubel, P. H. E. Smeets, J. G. P. Peters, R. J. M. Bindels, F. G. M. Russel, The MRP4/ABCC4 gene encodes a novel apical organic anion transporter in human kidney proximal tubules: Putative efflux pump for urinary cAMP and cGMP. *J. Am. Soc. Nephrol.* **13**, 595–603 (2002).
44. J. E. Souness, S. Rao, Proposal for pharmacologically distinct conformers of PDE4 cyclic AMP phosphodiesterases. *Cell. Signal.* **9**, 227–236 (1997).
45. S. D. Boomkamp, M. A. McGrath, M. D. Houslay, S. C. Barnett, Epac and the high affinity rolipram binding conformer of PDE4 modulate neurite outgrowth and myelination using an in vitro spinal cord injury model. *Br. J. Pharmacol.* **171**, 2385–2398 (2014).
46. M. S. Barnette *et al*., Inhibitors of phosphodiesterase IV (PDE IV) increase acid secretion in rabbit isolated gastric glands: correlation between function and interaction with a high-affinity rolipram binding site. *J. Pharmacol. Exp. Ther.* **273**, 1396–1402 (1995).
47. M. S. Barnette *et al*., SB 207499 (Ariflo), a potent and selective second-generation phosphodiesterase 4 inhibitor: In vitro anti-inflammatory actions. *J. Pharmacol. Exp. Ther.* **284**, 420–426 (1998).
48. H. -T. Zhang *et al*., Antidepressant-like effects of PDE4 inhibitors mediated by the high-affinity rolipram binding state (HARBS) of the phosphodiesterase-4 enzyme (PDE4) in rats. *Psychopharmacol. (Berl).* **186**, 209–217 (2006).
49. Y. Zhao, H.-T. Zhang, J. M. O'Donnell, Inhibitor binding to type 4 phosphodiesterase (PDE4) assessed using [^{3}H]Piclamilast and [^{3}H]. *Rolipram.* **305**, 565–572 (2003).
50. I. McPhee *et al*., Association with the SRC family tyrosyl kinase LYN triggers a conformational change in the catalytic region of human cAMP-specific phosphodiesterase HSPDE4A4B. Consequences for rolipram inhibition. *J. Biol. Chem.* **274**, 11796–11810 (1999).
51. R. Alvarez *et al*., Activation and selective inhibition of a cyclic AMP-specific phosphodiesterase, PDE-4D3. *Mol. Pharmacol.* **48**, 616–622 (1995).
52. B. Buchholz, B. Teschemacher, G. Schley, H. Schillers, K. U. Eckardt, Formation of cysts by principal-like MDCK cells depends on the synergy of cAMP- and ATP-mediated fluid secretion. *J. Mol. Med. (Berl.)* **89**, 251–261 (2011).
53. S. Rees *et al*., Adenylyl cyclase 6 deficiency ameliorates polycystic kidney disease. *J. Am. Soc. Nephrol.* **25**, 232–237 (2014).
54. Q. Wang *et al*., Adenylyl cyclase 5 deficiency reduces renal cyclic AMP and cyst growth in an orthologous mouse model of polycystic kidney disease. *Kidney Int.* **93**, 403–415 (2018).
55. S. Terryn, A. Ho, R. Beauwens, O. Devuyst, Fluid transport and cystogenesis in autosomal dominant polycystic kidney disease. *Biochim. Biophys. Acta* **1812**, 1314–1321 (2011).
56. E. Blanchard *et al*., Anchored PDE4 regulates chloride conductance in wild-type and ΔF508-CFTR human airway epithelia. *FASEB J.* **28**, 791–801 (2014).
57. J. A. Lambert *et al*., Cystic fibrosis transmembrane conductance regulator activation by roflumilast contributes to therapeutic benefit in chronic bronchitis. *Am. J. Respir. Cell Mol. Biol.* **50**, 549–558 (2014).
58. H. Li, I. A. Findlay, D. N. Sheppard, The relationship between cell proliferation, Cl^- secretion, and renal cyst growth: A study using CFTR inhibitors. *Kidney Int.* **66**, 1926–1938 (2004).
59. B. Yang, N. D. Sonawane, D. Zhao, S. Somlo, A. S. Verkman, Small-molecule CFTR inhibitors slow cyst growth in polycystic kidney disease. *J. Am. Soc. Nephrol.* **19**, 1300–1310 (2008).
60. W. V. Breuer, E. Mack, A. Rothstein, Activation of K^+ and Cl^- channels by Ca^{2+} and cyclic AMP in dissociated kidney epithelial (MDCK) cells. *Pflugers Arch.* **411**, 450–455 (1988).
61. A. J. Streets *et al*., Parallel microarray profiling identifies ErbB4 as a determinant of cyst growth in ADPKD and a prognostic biomarker for disease progression. *Am. J. Physiol. Renal. Physiol.* **312**, F577–F588 (2017).
62. C. D'Sa, L. M. Tolbert, M. Conti, R. S. Duman, Regulation of cAMP-specific phosphodiesterases type 4B and 4D (PDE4) splice variants by cAMP signaling in primary cortical neurons. *J. Neurochem.* **81**, 745–757 (2002).
63. I. R. Le Jeune, M. Shepherd, G. Van Heeke, M. D. Houslay, I. P. Hall, Cyclic AMP-dependent transcriptional up-regulation of phosphodiesterase 4D5 in human airway smooth muscle cells: Identification and characterization of a novel PDE4D5 promoter. *J. Biol. Chem.* **277**, 35980–35989 (2002).
64. Y. H. Choi *et al*., Polycystin-2 and phosphodiesterase 4C are components of a ciliary A-kinase anchoring protein complex that is disrupted in cystic kidney diseases. *Proc. Natl. Acad. Sci. U.S.A.* **108**, 10679–10684 (2011).
65. D. Willoughby *et al*., Dynamic regulation, desensitization, and cross-talk in discrete subcellular microdomains during beta2-adrenoceptor and prostanoid receptor cAMP signaling. *J. Biol. Chem.* **282**, 34235–34249 (2007).
66. M. B. Beard *et al*., UCR1 and UCR2 domains unique to the cAMP-specific phosphodiesterase family form a discrete module via electrostatic interactions. *J. Biol. Chem.* **275**, 10349–10358 (2000).
67. A. B. Burgin *et al*., Design of phosphodiesterase 4D (PDE4D) allosteric modulators for enhancing cognition with improved safety. *Nat. Biotechnol.* **28**, 63–70 (2010).
68. J. P. Day *et al*., Elucidation of a structural basis for the inhibitor-driven, p62 (SQSTM1)-dependent intracellular redistribution of cAMP phosphodiesterase-4A4 (PDE4A4). *J. Med. Chem.* **54**, 3331–3347 (2011).
69. T. V. Masyuk, A. I. Masyuk, N. F. La Russo, Therapeutic targets in polycystic liver disease. *Curr. Drug Targets* **18**, 950–957 (2017).
70. M. J. Lynch *et al*., RNA silencing identifies PDE4D5 as the functionally relevant cAMP phosphodiesterase interacting with beta arrestin to control the protein kinase A/AKAP79-mediated switching of the beta2-adrenergic receptor to activation of ERK in HEK293B2 cells. *J. Biol. Chem.* **280**, 33178–33189 (2005).
71. C. S. Pinto *et al*., Phosphodiesterase isoform regulation of cell proliferation and fluid secretion in autosomal dominant polycystic kidney disease. *J. Am. Soc. Nephrol.* **27**, 1124–1134 (2016).
72. R. J. Marchmont, M. D. Houslay, A peripheral and an intrinsic enzyme constitute the cyclic AMP phosphodiesterase activity of rat liver plasma membranes. *Biochem. J.* **187**, 381–392 (1980).
73. G. B. Bolger *et al*., Characterization of five different proteins produced by alternatively spliced mRNAs from the human cAMP-specific phosphodiesterase PDE4D gene. *Biochem. J.* **328**, 539–548 (1997).
74. D. J. Henderson *et al*., The cAMP phosphodiesterase-4D7 (PDE4D7) is downregulated in androgen-independent prostate cancer cells and mediates proliferation by compartmentalising cAMP at the plasma membrane of VCaP prostate cancer cells. *Br. J. Cancer* **110**, 1278–1287 (2014).
75. R. Maitra, P. Sivashanmugam, K. Warner, A rapid membrane potential assay to monitor CFTR function and inhibition. *J. Biomol. Screen.* **18**, 1132–1137 (2013).